Expansion of Shockley stacking fault observed by scanning electron microscope and partial dislocation motion in 4H-SiC

Yoshifumi Yamashita, Ryu Nakata, Takeshi Nishikawa, Masaki Hada, and Yasuhiko Hayashi
Graduate School of Natural Science and Technology, Okayama University, 3-1-1, Tsushima-naka, Kita-ku, Okayama 700-8530, Japan

(Received 27 October 2017; accepted 21 December 2017; published online 30 January 2018)

We studied the dynamics of the expansion of a Shockley-type stacking fault (SSF) with 30° Si(g) partial dislocations (PDs) using a scanning electron microscope. We observed SSFs as dark lines (DLs), which formed the contrast at the intersection between the surface and the SSF on the (0001) face inclined by 8° from the surface. We performed experiments at different electron-beam scanning speeds, observing magnifications, and irradiation areas. The results indicated that the elongation of a DL during one-frame scanning depended on the time for which the electron beam irradiated the PD segment in the frame of view. From these results, we derived a formula to express the velocity of the PD using the elongation rate of the corresponding DL during one-frame scanning. We also obtained the result that the elongation velocity of the DL was not influenced by changing the direction in which the electron beam irradiates the PD. From this result, we deduced that the geometrical kink motion of the PD was enhanced by diffusing carriers that were generated by the electron-beam irradiation. *Published by AIP Publishing.* https://doi.org/10.1063/1.5010861

INTRODUCTION

4H-SiC is a promising material for power devices that may replace silicon. Schottky diodes and metal-oxide silicon field-effect transistors (MOSFETs) have already been put to practical use and are commercially available. However, it is necessary to fabricate bipolar devices with high breakdown voltage in order to utilize the prominent physical properties of 4H-SiC. Currently, this is impeded by the formation and expansion of Shockley-type stacking faults (SSFs) during forward-bias operation in bipolar devices, which significantly increases the resistance to forward current.[1,2] Therefore, this phenomenon has drawn the attention of researchers, and many works have been reported.[3] It was recently reported that SSF expansion was successfully suppressed by using a buffer layer with a short minority-carrier lifetime in which SSFs were confined at the beginning of epitaxial growth.[4,5] This could be an effective method, but it may not suppress SSF formation during the post-growth process. Controlling the expansion of SSFs is still an important area of research.

On the other hand, such systems are interesting from the viewpoint of fundamental research on the dislocation dynamics in four-valent semiconductors. The SSF expansion in 4H-SiC is induced by the inversion of the SSF formation energy to the negative sign by electron trapping (and holes as excitons), in addition to the enhanced mobility of 30° partial dislocations (PDs) with Si core atoms in the glide-set core structure (30° Si(g) PDs), which form the leading edge of the SSF.[6–12] Such enhancement of PD motion is widely observed in semiconductors and is known as radiation-enhanced dislocation glide (REDG).[13] There are some reports on the REDG effect in 4H-SiC. Galeckas *et al.* reported the temperature dependence of PD velocities under laser illumination, where the activation energy of enhanced PD motion was reduced to 0.25 eV,[14] whereas that in the dark was reported as 1.7 eV.[15] Dislocation glide motion is a complex process consisting of kink-pair formation and kink migration. Ohno *et al.* observed the motion of PDs with a transmission electron microscope (TEM) and found that the kink migration was enhanced by electron irradiation.[16] The mechanism of the REDG effect in semiconductors has been explained as a recombination-enhanced defect reaction (REDR).[13,17] Hirano *et al.* recently claimed that the mechanism of REDG in 4H-SiC is not REDR but the photoionization of dislocations by laser illumination, based on their experiments.[18] However, there are a few research reports on the REDG effects of PD in 4H-SiC, and many fundamental areas remain to be explored.

Previous research on SSF expansion or PD motion often employed imaging methods using electroluminescence,[11] photoluminescence,[14,18,19] cathodoluminescence,[20] or electron-beam-induced current.[20,21] In this paper, we report the observation of SSFs using secondary electron images, which is the most common mode of scanning electron microscopy (SEM) operation. We observed the intersecting line between an SSF and the surface as a dark line (DL). This contrast may be attributed to the high conductivity at the SSF that forms a two-dimensional quantum well. The probe beam of the SEM plays the dual roles of minority-carrier excitation and imaging of the SSF. The velocity of a 30° Si(g) PD should be obtained from the elongation rate of the DL. We examined the characteristics of DL elongation and derived an expression of PD velocity. We also report some fundamental information on the mechanism of the REDG effect in 4H-SiC.

EXPERIMENTAL

We used an n-type 4H-SiC (0001) epi-wafer whose [0001] axis was tilted at 8° toward the [11 − 20] direction around the [1 − 100] axis as the rotation axis. The resistivity of the substrate was 0.02 Ωcm. Both a buffer layer of 0.5 μm

and an epi-layer of 8 μm were grown, and each layer was doped with nitrogen at $1.0 \times 10^{18}\,\mathrm{cm}^{-3}$ and $2.4 \times 10^{16}\,\mathrm{cm}^{-3}$, respectively. The [11 − 20] direction was defined as directing the epi-surface from the substrate in the (0001) plane.

In this study, the observations of SSF and concurrent electron-beam irradiation were performed by an SEM with an acceleration voltage of 30 kV. The SEM was equipped with a LaB_6 filament. The objective aperture was removed during irradiation in order to gain more electron flux. Unfortunately, the irradiation current was not known due to the lack of a Faraday cup. Therefore, once the filament was on and the beam alignment was adjusted, the series of experiments was completed without changing the irradiation conditions.

A scratch was introduced on the epi-surface by a diamond stylus with 5 g loading in the [11 − 20] direction in order to introduce the sources of SSFs. The sample was oriented so that the scratch could be observed vertically in the SEM image. The sample was irradiated mainly on the right side of the scratch using slow-scan modes. As we repeated the irradiation near the scratch, we observed that dark lines (DLs) grew to extend from the vicinity of the scratch. The DL is the intersection line between an SSF and the epi-surface. Such an expansion of SSFs at room temperature is known to occur through the glide motion of 30° Si(g) PDs with an enhanced mobility under electronic excitation.[8] Since a 30° Si(g) PD should be extending from the front of the DL toward the inside of the crystal, we can measure the velocity of the 30° Si(g) PD, which cannot be directly observed in SEM images by tracking the elongation of the DL attributed to the SSF. Figure 1 shows a schematic representing a DL and its associated SSF in the sample. We ensured that only a single SSF was formed in the field of view by gradually shifting the view frame away from the scratch. We thus measured the elongation rate of the DL.

RESULTS

We repeated one-frame scanning with the SEM using the slow-scan mode for electron-beam irradiation and recording the image. Figures 2(a)–2(c) show a typical sequentially recorded set of SEM images. The square dark contrast on the left side of each image and the short curves extending from the right side of the dark square are traces that had been previously irradiated, and they are not of our interest here. The horizontal DL indicated by the white arrow is the line of intersection between the SSF and the epi-surface. A careful observation reveals that the DLs are imaged actually as stripes with some thickness, and the right end of the DL stripes is not vertical but is tilted to the right. This suggests that the SSF spreading in the crystal toward the upper side of the DL is bound by a 30° Si(g) PD, which extends in the oblique direction as shown in Fig. 1.

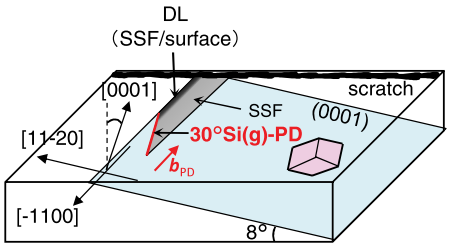

FIG. 1. Schematic showing the direction of the sample and a DL associated with an SSF. The red line represents a 30° Si(g) PD, which forms the front edge of the SSF. The Burgers vector of the PD ($\boldsymbol{b}_{PD}$) is shown by a red arrow.

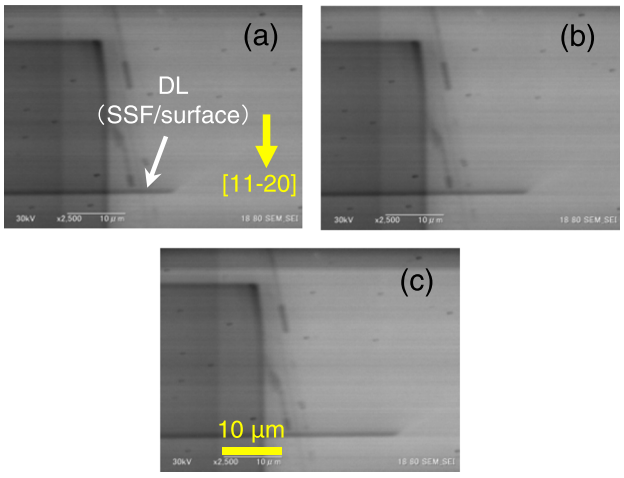

FIG. 2. Typical sequentially recorded SEM images. The horizontal DL, as indicated by the white arrow, is due to the line of intersection between the SSF and the epi-surface.

The extension of DL (X) due to an SSF increased by the same length for every one-frame irradiation in Fig. 2. These experiments were performed using the slow-scan mode 2 at the rate of 8.3 s/f (seconds per frame) and mode 3 at 16.7 s/f. The results are shown in Fig. 3. The DL extends at a constant rate for each scan, and doubling the scanning time for a frame doubles the elongation rate of the DL.

Figure 4 shows the dependence of the elongation of a DL on the magnification of the SEM observation. We can see that the elongation of the DL for one-frame irradiation (ΔX) is approximately proportional to the square of the magnification. The irradiation area decreases in inverse proportion to the 2nd power of the magnification, whereas the scanning time of a frame in this experiment is constant regardless of the magnification. Therefore, the time for irradiating a specific area is proportional to the 2nd power of the magnification. From these facts and results, shown in Figs. 3 and 4, the elongation rate of the DL is proportional to the irradiation time for a specific area. Because the elongation of

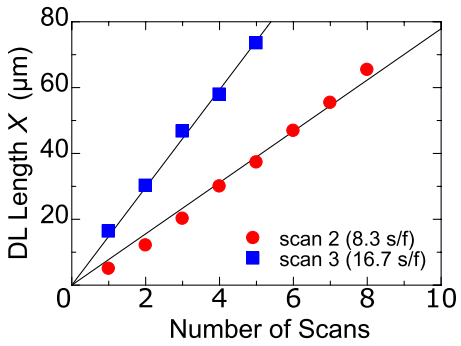

FIG. 3. Elongation of the DL by every one-frame scan in slow-scan mode 2 (8.3 s/f, closed circle) and mode 3 (16.7 s/f, closed square). The slope of the fitted lines is 7.8 μm/f for scan 2 and 15 μm/f for scan 3.

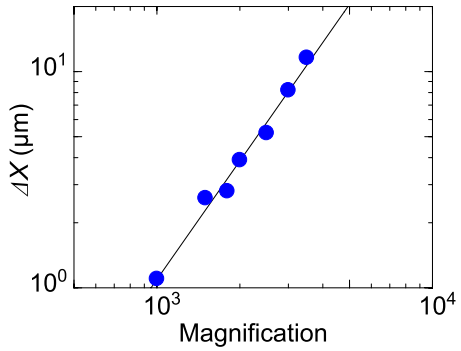

FIG. 4. Magnification dependence of the elongation of the DL (ΔX) for one-frame scanning. The slope of the fitted line is 1.8.

a DL corresponds to the travel distance of a 30° Si(g) PD near the surface, the elongation rate of a DL must be proportional to the time for irradiating the PD rather than the time for irradiating the area. Accordingly, we performed additional experiments to measure ΔX by changing the vertical position of the DL (L) measured from the top of the field of view. Here, we assume that the SSF had extended down to the buffer/epi-layer boundary. Since the electrons reach the SSF plane that is all the way shallow enough from the surface as shown later in "Discussion," the variable L represents the width of the SSF under electron irradiation and hence is equal to half of the length of the 30° Si(g) PD irradiated with electrons. To ensure this condition, we paid attention so that the PD segment extending in the direction of 30° from the end of the DL would not extend out from the right side of the field of view but from the top side of it. Figure 5 shows the resulting linear dependence of ΔX on L. This result clearly shows that the elongation of the DL is proportional to the irradiation time for the whole part of PD segment in the field of view. This means that the near-surface portion of the PD is traveling, while other portions apart from the surface are being irradiated. In other words, the elongation of the DL during one-frame irradiation is the accumulation of the displacements of the parts of the PD being irradiated during the scanning electron beam. We note that the DL did not elongate when $L \sim 0$ although the minority carriers may diffuse over tens of microns. This means that PD motion is not enhanced only by diffusing minority carriers. The good linearity in Fig. 5 also implies that the depth profile of electronic excitation is approximately uniform.

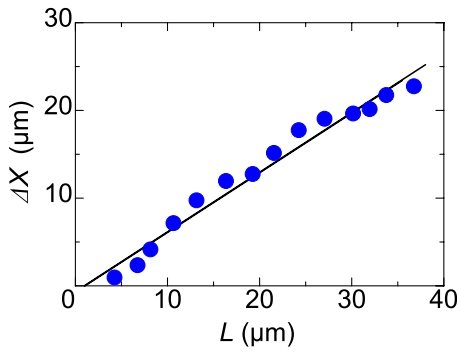

FIG. 5. Relationship between the vertical position of the DL (L) and ΔX. These data were taken under the condition of scan mode 3 and 1200× magnification.

A matter of concern might be the sequential order of the DL drawing instance in the SEM image and the time when the connecting 30° Si(g) PD is irradiated. Because the electron beam is scanned from the top to the bottom in the field of view, the DL is drawn after the corresponding PD is irradiated in the case where [11 − 20] is directed downward, as shown in Fig. 2. On the other hand, the PD is irradiated after the DL is drawn if the sample is set, whereby [11 − 20] is directed upward in the field of view. Therefore, ΔX for the latter case is the traveling distance during the previous scanning of the frame. We investigated whether there is any difference between the two cases, one in which the scanning raster line of the electron-beam moves in the [11 − 20] direction and the other in the opposite [-1 − 120] direction. Because the moving direction of the raster line could not be changed, the sample was rotated by 180° to reverse the irradiation order, and ΔX was examined for the identical DL. Here, the scanning speed of the probe beam for one-line sweeping is much faster than the 30° Si(g) PD motion that is estimated later, such that the effect of inverting the direction of the probe beam motion in one-line sweeping is negligible. The results are shown in Fig. 6. We cannot see any difference between the two cases.

DISCUSSION

From the experimental results, the formula to evaluate the velocity of a 30° Si(g) PD under electron-beam irradiation was derived as follows: To help in understanding the situation, a schematic of a view frame and a PD that is not seen in the SEM image is shown in Fig. 7. If we let R be the radius of the electron range where the electron-hole pair is formed by electron-beam irradiation, the time for a point on a 30° Si(g) PD to be irradiated during one-frame scanning is given by

$$\Delta t = \frac{(2R)^2}{WH} T, \tag{1}$$

where W and H represent the width and height of the view frame, respectively, and T represents the scanning time for a frame. We note that Eq. (1) is valid as far as the raster line spacing (actually $<= 0.2\,\mu$m in our experimental condition)

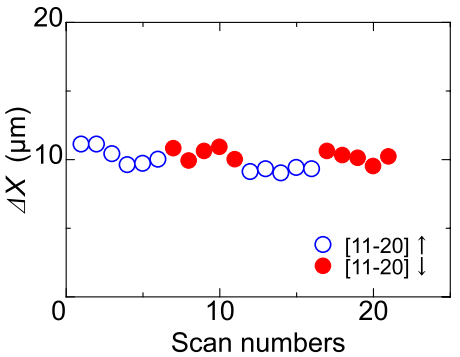

FIG. 6. Elongation of the DL for one-frame irradiation ΔX in the case where the direction of vertical movement of the scanning line was inverted. The results where the [11 − 20] direction is downward on the screen, as shown in Fig. 2, are represented by closed circles and the case where the [11 − 20] direction is upward by open circles.

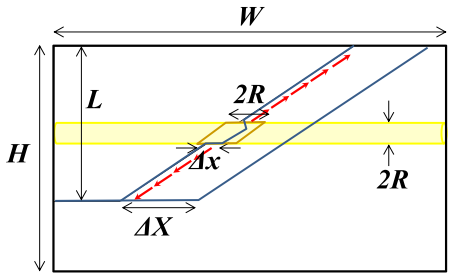

FIG. 7. Schematic of a SSF associated with a DL and a 30° Si(g) PD in a view frame. A band of the electron range corresponding to one raster line is also shown. A series of small arrows represents the motion of geometrical kinks enhanced by carriers diffusing out from the electron range.

is narrower than R. When the traveling distance of the irradiated PD in the infinitesimal length is Δx, the observed elongation of the DL for one-frame irradiation ΔX is given as follows considering that ΔX is the accumulation of the displacements Δx of infinitesimal segments of PD, as already deduced from the results shown in Fig. 5

$$\Delta X = \frac{L}{2R}\Delta x. \tag{2}$$

Therefore, the velocity of the 30° Si(g) PD under irradiation is expressed as

$$v = \frac{\Delta x}{\Delta t} = \frac{WH}{2RL}\frac{\Delta X}{T}. \tag{3}$$

The magnitude of R is estimated to be approximately 3.3 μm.[22] Using our experimental value of $\Delta X/L$, the velocity v of the PD in Fig. 5 is evaluated to be approximately 5×10^{-5} m/s. Using this value and the lateral moving speed of the electron probe ($<= 3 \times 10^{-3}$ m/s), the magnitude of Δx for a line scan at the largest is estimated to be approximately 0.1 μm, which is sufficiently smaller than R. Therefore, it is confirmed that Δx was not given by R. The obtained PD velocity, 5×10^{-5} m/s, corresponds to the velocity in the case of irradiation at 1.2×10^{6} W/cm^2, from the results shown in the literature.[19] The irradiation current was not measured in our experiments, but the estimated current from this power is approximately 4 μA, which is roughly plausible.

As illustrated in Fig. 7, there must be accumulation of kinks (geometrical kinks) on both sides of the bump which bounds the PD segment that is already advanced by Δx under irradiation and the segment that is not irradiated. The DL in the SEM image continued to elongate at a constant rate, as shown in Fig. 2. This fact implies that the PD at the end of the DL continued to be in a linear shape tilting at an angle of about 30° although the whole segment of the PD was not visible in the SEM image. Maeda *et al.* observed the linear shape of the leading edge of SSFs after the line scan of the laser beam by photoluminescence.[12] This situation of keeping the PD orientation is achieved by the fast migration of geometrical kinks on the whole PD segment. However, geometrical kinks are not considered to move thermally at room temperature because the migration barrier is reported to be as large as, for example, 1.85 eV.[23] Therefore, the migration of geometrical kinks is due to the enhancement effect of the electron-beam irradiation. This is consistent with a previous report based on the TEM observation of 30° Si(g) PD motion.[16] In that report, it was also inferred that the enhanced mobility of the left and right kinks is asymmetric, from the fact that the PD direction is always shifted to one side in the direction of Peierls potential. Our results, however, did not indicate such asymmetry of kink motion, which is deduced from the results shown in Fig. 6. The inversion of the moving direction of the raster line makes the inversion of the sign (left or right) of geometrical kinks relevant to the elongation of the DL. However, the elongation of the DL showed no difference between the two cases, as shown in Fig. 6. The reason for this discrepancy is not clear at present.

Hirano *et al.* reported that the mechanism of the REDG effect is photoionization of the dislocation, based on the analysis of their experimental results of irradiating laser light on the portion of 30° Si(g) PD at various depths from the surface.[18] The motion of geometrical kink was also enhanced on those parts of the PD which were not irradiated, which was clearly shown in our experiments. Therefore, the enhancement of kink migration can be induced by carriers diffusing in the crystal from the irradiated area. Because such thermalized carriers do not ionize kinks, the enhancement of kink motion should be caused by the recombination of excited carriers, which has been widely believed. In the excited region that is the electron range in the case of electron-beam irradiation, both kink-pair formation and kink migration occur. Because the kink migration is enhanced by the REDR mechanism, the process enhanced by the ionization mechanism must be the kink-pair formation process. We speculate that the level ionized by irradiation is not the level associated with the kink but another level on the straight dislocation line, such as a soliton site, which may be relevant to the kink-pair formation.[24,25] This speculation should be confirmed by future study. At least in this system, both kink-pair formation and kink migration are enhanced by the electronic excitation, and the enhancing mechanism for each process is different from each other.

CONCLUSION

We investigated the SSF expansion induced by a 30° Si(g) PD glide motion under the irradiation of a scanning electron beam using an SEM. We showed that the length of the PD in the field of view is an important parameter to calculate the velocity of the PD motion from the DL elongation rate and that we could obtain the velocity of the PD motion. The obtained velocity is roughly comparable to that reported in the literature. These findings ensure the validity of the formula that we present in this paper. We also showed that the kink migration is enhanced by the diffusing carriers created by the irradiation, and this enhancement is attributed to the conventional REDR mechanism.

[1]H. Lendenmann, F. Dahquist, N. Johansson, R. Söderholm, P. A. Nilsson, J. P. Bergmann, and P. Skytt, Mater. Sci. Forum **353–356**, 727 (2001).
[2]J. P. Bergman, H. Lendenmann, P. Å. Nilsson, U. Lindefelt, and P. Skytt, Mater. Sci. Forum **353–356**, 299 (2001).
[3]M. Skowronski and S. Ha, J. Appl. Phys. **99**, 011101 (2006).
[4]T. Tawara, T. Miyazawa, M. Ryo, M. Miyazato, T. Fujimoto, K. Takenaka, S. Matsunaga, M. Miyajima, A. Otsuki, Y. Yonezawa, T. Kato,

H. Okumura, T. Kimoto, and H. Tsuchida, J. Appl. Phys. **120**, 115101 (2016).
[5]T. Miyazawa, T. Tawara, R. Takanashi, and H. Tsuchida, Appl. Phys. Express **9**, 111301 (2016).
[6]M. S. Miao, S. Limpijumnong, and W. R. L. Lambrecht, Appl. Phys. Lett. **79**, 4360 (2001).
[7]W. R. L. Lambrecht and M. S. Miao, Phys. Rev. B **73**, 155312 (2006).
[8]S. Ha, M. Benamara, M. Skowronski, and H. Lendenmann, Appl. Phys. Lett. **83**, 4957 (2003).
[9]S. Ha and M. Skowronski, Phys. Rev. Lett. **92**, 175504 (2004).
[10]J. D. Caldwell, R. E. Stahlbush, M. G. Ancona, O. J. Glembocki, and K. D. Hobart, J. Appl. Phys. **108**, 044503 (2010).
[11]A. Galeckas, J. Linnros, and P. Pirouz, Appl. Phys. Lett. **81**, 883 (2002).
[12]K. Maeda, R. Hirano, Y. Sato, and M. Tajima, Mater. Sci. Forum **725**, 35 (2012).
[13]K. Maeda and S. Takeuchi, in *Dislocations in Solids*, edited by F. R. N. Nabarro and M. S. Duesbery (North-Holland, Amsterdam, 1996), Vol. 10, p. 443.
[14]A. Galeckas, J. Linnros, and P. Pirouz, Phys. Rev. Lett. **96**, 025502 (2006).
[15]H. Idrissi, B. Pichaud, G. Regula, and M. Lancin, J. Appl. Phys. **101**, 113533 (2007).
[16]Y. Ohno, I. Yonenaga, K. Miyao, K. Maeda, and H. Tsuchida, Appl. Phys. Lett. **101**, 042102 (2012).
[17]J. D. Weeks, J. C. Tully, and L. C. Kimerling, Phys. Rev. B **12**, 3286 (1975).
[18]R. Hirano, Y. Sato, H. Tsuchida, M. Tajima, K. M. Ito, and K. Maeda, Appl. Phys. Express **5**, 091302 (2012).
[19]R. Hirano, Y. Sato, M. Tajima, K. M. Ito, and K. Maeda, Mater. Sci. Forum **717–720**, 395 (2012).
[20]E. B. Yakimov, G. Regula, and B. Pichaud, J. Appl. Phys. **114**, 084903 (2013).
[21]B. Chen, H. Matsuhata, T. Sekiguchi, T. Ohyanagi, A. Kinoshita, and H. Okumura, Appl. Phys. Lett. **96**, 212110 (2010).
[22]T. E. Everhart and P. H. Hoff, J. Appl. Phys. **42**, 5837 (1971).
[23]G. Savini, M. I. Heggie, and S. Öberg, New J. Phys. **9**, 6 (2007).
[24]M. Heggie and R. Jones, Philos. Mag. B **48**, 365 (1983).
[25]K. Maeda, K. Suzuki, Y. Yamashita, and Y. Mera, J. Phys.: Condens. Matter. **12**, 10079 (2000).